arXiv:astro-ph/0007253v1 18 Jul 2000

Dirac equation in Kerr geometry and its solution

Sandip K. Chakrabarti([1]) and Banibrata Mukhopadhyay([1])

([1]) *S. N. Bose National Centre for Basic Sciences, JD-Block, Sector III, Salt Lake, Calcutta 700091, India emails: chakraba@boson.bose.res.in and bm@boson.bose.res.in*

Summary. —
Chandrasekhar separated the Dirac equation for spinning and massive particles in Kerr geometry into radial and angular parts. In the present review, we present solutions of the complete wave equation and discuss how the Dirac wave scatters off Kerr black holes. The eigenfunctions, eigenvalues and reflection and transmission coefficients are computed for different Kerr parameters. We compare the solutions with several parameters to show how a spinning black hole distinguishes mass and energy of incoming waves. Very close to the horizon, the solutions become independent of the particle parameters indicating an universality of the behaviour.

PACS 04.20.-q – Classical general relativity.
PACS 04.70.-s – Physics of black holes.
PACS 04.70.Dy – Quantum aspects of black holes.
PACS 95.30.Sf – Relativity and gravitation.

Il Nuovo Cimento (in press)

1. – Introduction

One of the most important solutions of Einstein's equation is that of the spacetime around and inside an isolated black hole. The spacetime at a large distance is flat and Minkowskian where usual quantum mechanics is applicable, while the spacetime closer to the singularity is so curved that no satisfactory quantum field theory could be developed as yet. An intermediate situation arises when a weak perturbation (due to, say, gravitational, electromagnetic or Dirac waves) originating from infinity interacts with a black hole. The resulting wave is partially transmitted into the black hole through the horizon and partially scatters off to infinity. In the linearized ('test field') approximation this problem has been attacked in the past by several authors [1, 2, 3, 4]. The master equations of Teukolsky [2] which govern these linear perturbations for integral spin (e.g., gravitational and electromagnetic) fields were solved numerically by Press & Teukolsky [5] and Teukolsky & Press [6]. While the equations governing the massive Dirac particles were separated in 1976 [3], the angular eigenfunction and eigenvalue (which happens to be the separation constant) have been obtained in 1984 [7] and radial solutions have

© Società Italiana di Fisica

been obtained only recently [8, 9, 10, 11]. Particularly interesting is the fact that whereas gravitational and electromagnetic radiations were found to be amplified in some range of incoming frequencies, Chandrasekhar [4] predicted that no such amplifications should take place for Dirac waves because of the very nature of the potential experienced by the incoming fields. Although this later conclusion was drawn using an asymptotic equation, we show that this is indeed the case even when complete solutions are considered for the Dirac wave perturbations. Chandrasekhar also speculated that one needs to look into the problem for negative eigenvalues (λ) where one *might* come across super-radiance for Dirac waves.

In the present review, we discuss this important problem and its solutions. We show the nature of the radial wave functions as a function of the Kerr parameter, rest mass and frequency of incoming particle. We also verify that super-radiance is indeed absent for the Dirac field. Unlike earlier works [5, 6] where numerical (shooting) methods were used to solve the master equations governing gravitational and electromagnetic waves, we use a classical approach whereby we approximate the potential felt by the particle by a collection of small steps.

Below, we present the separated Dirac equations from Chandrasekhar [4] using the same choice of units: we choose $\hbar = 1 = G = c$, so that the unit of mass becomes $\sqrt{\frac{\hbar c}{G}}$, the unit of time becomes $\sqrt{\frac{\hbar G}{c^5}}$, and the unit of length becomes $\sqrt{\frac{\hbar G}{c^3}}$.

The equations governing the radial wave-functions $R_{\pm\frac{1}{2}}$ corresponding to spin $\pm\frac{1}{2}$ respectively are given by:

$$\Delta^{\frac{1}{2}}\mathcal{D}_0 R_{-\frac{1}{2}} = (\lambda + im_p r)\Delta^{\frac{1}{2}} R_{+\frac{1}{2}}, \tag{1a}$$

$$\Delta^{\frac{1}{2}}\mathcal{D}_0^\dagger \Delta^{\frac{1}{2}} R_{+\frac{1}{2}} = (\lambda - im_p r) R_{-\frac{1}{2}}, \tag{1b}$$

where, the operators $\mathcal{D}_n$ and $\mathcal{D}_n^\dagger$ are given by,

$$\mathcal{D}_n = \partial_r + \frac{iK}{\Delta} + 2n\frac{(r-M)}{\Delta}, \tag{2a}$$

$$\mathcal{D}_n^\dagger = \partial_r - \frac{iK}{\Delta} + 2n\frac{(r-M)}{\Delta}, \tag{2b}$$

and

$$\Delta = r^2 + a^2 - 2Mr, \tag{3a}$$

$$K = (r^2 + a^2)\sigma + am. \tag{3b}$$

Here, a is the Kerr parameter, n is an integer or half integer, σ is the frequency of incident wave, M is the mass of the black hole, m_p is the rest mass of the Dirac particle, λ is the eigenvalue of the Dirac equation and m is the azimuthal quantum number.

The equations governing the angular wave-functions $S_{\pm\frac{1}{2}}$ corresponding to spin $\pm\frac{1}{2}$ respectively are given by:

$$\mathcal{L}_{\frac{1}{2}} S_{+\frac{1}{2}} = -(\lambda - am_p \cos\theta) S_{-\frac{1}{2}} \tag{4a}$$

$$\mathcal{L}^{\dagger}_{\frac{1}{2}} S_{-\frac{1}{2}} = +(\lambda + am_p \cos\theta) S_{+\frac{1}{2}} \tag{4b}$$

where, the operators $\mathcal{L}_n$ and $\mathcal{L}^{\dagger}_n$ are given by,

$$\mathcal{L}_n = \partial_\theta + Q + n\cot\theta, \tag{5a}$$

$$\mathcal{L}^{\dagger}_n = \partial_\theta - Q + n\cot\theta \tag{5b}$$

and

$$Q = a\sigma\sin\theta + m \text{ cosec } \theta. \tag{6}$$

Note that both the radial and the angular sets of equations i.e., eqs. 1(a-b) and eqs. 4(a-b) are coupled equations. Combining eqs. 4(a-b), one obtains the angular eigenvalue equations for the spin-$\frac{1}{2}$ particles as [7]

$$\left[\mathcal{L}_{\frac{1}{2}}\mathcal{L}^{\dagger}_{\frac{1}{2}} + \frac{am_p\sin\theta}{\lambda + am_p\cos\theta}\mathcal{L}^{\dagger}_{\frac{1}{2}} + (\lambda^2 - a^2m_p^2\cos^2\theta)\right] S_{-\frac{1}{2}} = 0. \tag{7}$$

There are exact solutions of this equation for the eigenvalues λ and the eigenfunctions $S_{-\frac{1}{2}}$ when $\rho = \frac{m_p}{\sigma} = 1$ in terms of the orbital quantum number l and azimuthal quantum number m. These solutions are [7]:

$$\lambda^2 = (l+\frac{1}{2})^2 + a\sigma(p+2m) + a^2\sigma^2\left[1 - \frac{y^2}{2(l+1)+a\sigma x}\right], \tag{8}$$

and

$${}_{\frac{1}{2}}S_{lm} = {}_{\frac{1}{2}}Y_{lm} - \frac{a\sigma y}{2(l+1)+a\sigma x}\,{}_{\frac{1}{2}}Y_{l+1m} \tag{9}$$

where,

$$p = F(l,l); \quad x = F(l+1,l+1); \quad y = F(l,l+1)$$

and

$$F(l_1,l_2) = [(2l_2+1)(2l_1+1)]^{\frac{1}{2}} < l_2 1 m 0 | l_1 m >$$

$$[< l_2 1\frac{1}{2}0|l_1\frac{1}{2} > +(-1)^{l_2-l} < l_2 1 m0|l_1 m > [< l_2 1\frac{1}{2}0|l_1\frac{1}{2} > +(-1)^{l_2-l}\rho\sqrt{2} < l_2 1 -\frac{1}{2}1|l_1\frac{1}{2} >]. \tag{10}$$

with $< ....|.. >$ are the usual Clebsh-Gordon coefficients. For other values of ρ one has to use perturbation theories. Solutions upto sixth order using perturbation parameter $a\sigma$ are given in Chakrabarti [7] and are not described here. The eigenfunctions λ are required to solve the radial equations which we do now.

The radial equations 1(a-b) are in coupled form. One can decouple them and express the equation either in terms of spin up or spin down wave functions $R_{\pm\frac{1}{2}}$ but the expression loses its transparency. It is thus advisable to use the approach of Chandrasekhar [4] by changing the basis and independent variable r to,

$$r_* = r + \frac{2Mr_+ + am/\sigma}{r_+ - r_-}\log\left(\frac{r}{r_+} - 1\right) - \frac{2Mr_- + am/\sigma}{r_+ - r_-}\log\left(\frac{r}{r_-} - 1\right) \quad (r > r_+). \tag{11}$$

where,

$$\frac{d}{dr_*} = \frac{\Delta}{\omega^2}\frac{d}{dr}; \qquad \omega^2 = r^2 + \alpha^2; \qquad \alpha^2 = a^2 + am/\sigma, \tag{12}$$

to transform the set of coupled equations 1(a-b) into two independent one dimensional wave equations given by:

$$\left(\frac{d}{dr_*} - i\sigma\right)P_{+\frac{1}{2}} = \frac{\Delta^{\frac{1}{2}}}{\omega^2}(\lambda - im_p r)P_{-\frac{1}{2}}; \qquad \left(\frac{d}{dr_*} + i\sigma\right)P_{-\frac{1}{2}} = \frac{\Delta^{\frac{1}{2}}}{\omega^2}(\lambda + im_p r)P_{+\frac{1}{2}}. \tag{13}$$

Here, $\mathcal{D}_0 = \frac{\omega^2}{\Delta}(\frac{d}{dr_*} + i\sigma)$ and $\mathcal{D}_0^\dagger = \frac{\omega^2}{\Delta}(\frac{d}{dr_*} - i\sigma)$ were used and wave functions were redefined as $R_{-\frac{1}{2}} = P_{-\frac{1}{2}}$ and $\Delta^{\frac{1}{2}}R_{+\frac{1}{2}} = P_{+\frac{1}{2}}$.

We are now defining a new variable,

$$\theta = tan^{-1}(m_p r/\lambda) \tag{14}$$

which yields,

$$\cos\theta = \frac{\lambda}{\sqrt{(\lambda^2 + m_p^2 r^2)}}, \quad \text{and} \quad \sin\theta = \frac{m_p r}{\sqrt{(\lambda^2 + m_p^2 r^2)}}$$

and

$$(\lambda \pm im_p r) = exp(\pm i\theta)\sqrt{(\lambda^2 + m_p^2 r^2)},$$

so the coupled equations take the form,

$$\left(\frac{d}{dr_*} - i\sigma\right)P_{+\frac{1}{2}} = \frac{\Delta^{\frac{1}{2}}}{\omega^2}(\lambda^2 + m_p^2 r^2)^{1/2}P_{-\frac{1}{2}}exp\left[-i\tan^{-1}\left(\frac{m_p r}{\lambda}\right)\right], \tag{15a}$$

and

$$\left(\frac{d}{dr_*} + i\sigma\right)P_{-\frac{1}{2}} = \frac{\Delta^{\frac{1}{2}}}{\omega^2}(\lambda^2 + m_p^2 r^2)^{1/2}P_{+\frac{1}{2}}exp\left[i\tan^{-1}\left(\frac{m_p r}{\lambda}\right)\right]. \tag{15b}$$

Then defining,

$$P_{+\frac{1}{2}} = \psi_{+\frac{1}{2}}\ exp\left[-\frac{1}{2}i\ tan^{-1}\left(\frac{m_p r}{\lambda}\right)\right] \tag{16a}$$

and

$$P_{-\frac{1}{2}} = \psi_{-\frac{1}{2}}\ exp\left[+\frac{1}{2}i\ tan^{-1}\left(\frac{m_p r}{\lambda}\right)\right], \tag{16b}$$

we obtain,

$$\frac{d\psi_{+\frac{1}{2}}}{dr_*} - i\sigma\left(1+\frac{\Delta}{\omega^2}\frac{\lambda m_p}{2\sigma}\frac{1}{\lambda^2+m_p^2r^2}\right)\psi_{+\frac{1}{2}} = \frac{\Delta^{\frac{1}{2}}}{\omega^2}(\lambda^2+m_p^2r^2)^{1/2}\psi_{-\frac{1}{2}} \tag{17a}$$

and

$$\frac{d\psi_{-\frac{1}{2}}}{dr_*} + i\sigma\left(1+\frac{\Delta}{\omega^2}\frac{\lambda m_p}{2\sigma}\frac{1}{\lambda^2+m_p^2r^2}\right)\psi_{-\frac{1}{2}} = \frac{\Delta^{\frac{1}{2}}}{\omega^2}(\lambda^2+m_p^2r^2)^{1/2}\psi_{+\frac{1}{2}}. \tag{17b}$$

Further choosing $\hat{r}_* = r_* + \frac{1}{2\sigma}\tan^{-1}(\frac{m_p r}{\lambda})$ so that $d\hat{r}_* = (1+\frac{\Delta}{\omega^2}\frac{\lambda m_p}{2\sigma}\frac{1}{\lambda^2+m_p^2r^2})dr_*$, the above equations become,

$$\left(\frac{d}{d\hat{r}_*} - i\sigma\right)\psi_{+\frac{1}{2}} = W\psi_{-\frac{1}{2}}, \tag{18a}$$

and

$$\left(\frac{d}{d\hat{r}_*} + i\sigma\right)\psi_{-\frac{1}{2}} = W\psi_{+\frac{1}{2}}. \tag{18b}$$

where,

$$W = \frac{\Delta^{\frac{1}{2}}(\lambda^2+m_p^2r^2)^{3/2}}{\omega^2(\lambda^2+m_p^2r^2)+\lambda m_p\Delta/2\sigma}. \tag{19}$$

Now letting $Z_\pm = \psi_{+\frac{1}{2}} \pm \psi_{-\frac{1}{2}}$ we can combine the differential equations to give,

$$\left(\frac{d}{d\hat{r}_*} - W\right)Z_+ = i\sigma Z_-, \tag{20a}$$

and

$$\left(\frac{d}{d\hat{r}_*} + W\right)Z_- = i\sigma Z_+. \tag{20b}$$

From these equations, we readily obtain a pair of independent one-dimensional wave equations,

$$\left(\frac{d^2}{d\hat{r}_*^{\,2}}+\sigma^2\right)Z_\pm = V_\pm Z_\pm. \tag{21}$$

where, $V_\pm = W^2 \pm \frac{dW}{d\hat{r}_*}$,

$$= \frac{\Delta^{\frac{1}{2}}(\lambda^2+m_p^2r^2)^{3/2}}{[\omega^2(\lambda^2+m_p^2r^2)+\lambda m_p\Delta/2\sigma]^2}[\Delta^{\frac{1}{2}}(\lambda^2+m_p^2r^2)^{3/2} \pm ((r-M)(\lambda^2+m_p^2r^2)+3m_p^2r\Delta)]$$

$$\mp\frac{\Delta^{\frac{3}{2}}(\lambda^2+m_p^2r^2)^{5/2}}{[\omega^2(\lambda^2+m_p^2r^2)+\lambda m_p\Delta/2\sigma]^3}[2r(\lambda^2+m_p^2r^2)+2m_p^2\omega^2r+\lambda m_p(r-M)/\sigma]. \tag{22}$$

One important point to note: the transformation of spatial co-ordinate r to r_* (and $\hat{r}_*$) is taken not only for mathematical simplicity but also for a physical significance. When r is chosen as the radial co-ordinate, the decoupled equations for independent waves show diverging behaviour. However, by transforming those in terms of r_* (and $\hat{r}_*$) we obtain well behaved functions. The horizon is shifted from $r = r_+$ to $\hat{r}_* = -\infty$ unless $\sigma \leq \sigma_s = -am/2Mr_+$ (eq. 11). In this connection, it is customary to define σ_c where $\alpha^2 = 0$ (eq. 13). Thus, $\sigma_c = -m/a$. If $\sigma \leq \sigma_s$, the super-radiation is expected [4].

2. – Solution Procedure

The choice of parameters is generally made in such a way that there is a significant interaction between the particle and the black hole, i.e., when the Compton wavelength of the incoming wave is of the same order as the outer horizon of the Kerr black hole. Similarly, the frequency of the incoming particle (or wave) should be of the same order as inverse of light crossing time of the radius of the black hole. These yield [8],

$$m_p \sim \sigma \sim [M+\sqrt(M^2-a^2)]^{-1}. \tag{23}$$

One can easily check from equation (22) that for $r \to \infty$ (i.e., $\hat{r}_* \to \infty$) $V_\pm \to m_p^2$. So the total energy of the physical particle should greater than square of its rest mass. So if we expand the total parameter space in terms of frequency of the particle (or wave), σ and rest mass of the particle, m_p, it is clear that 50% of total parameter space where $\sigma < m_p$ is unphysical (In this case, the energy is such that a particle released from a finite distance cannot go back to infinity after scattering.), and one need not study this region. Out of the total physical parameter space there are two cases of interest: (1) the waves do not 'hit' the potential barrier and (2) the waves do hit the potential barrier. To sole these potential problem first, we replace the potential barrier by a large number of steps as in the step-barrier problem in quantum mechanics. Fig. 1 shows one such example of the potential barrier [10] V_+ (Eq. 22) which is drawn for $a = 0.5$, $m_p = 0.8$ and $\sigma = 0.8$. In reality we use tens of thousands of steps with suitable variable widths so that the steps become indistinguishable from the actual function. The solution of Eq. 22 at nth step can be written as [14],

$$Z_{+,n} = A_n exp[ik_n\hat{r}_{*,n}] + B_n exp[-ik_n\hat{r}_{*,n}] \tag{24}$$

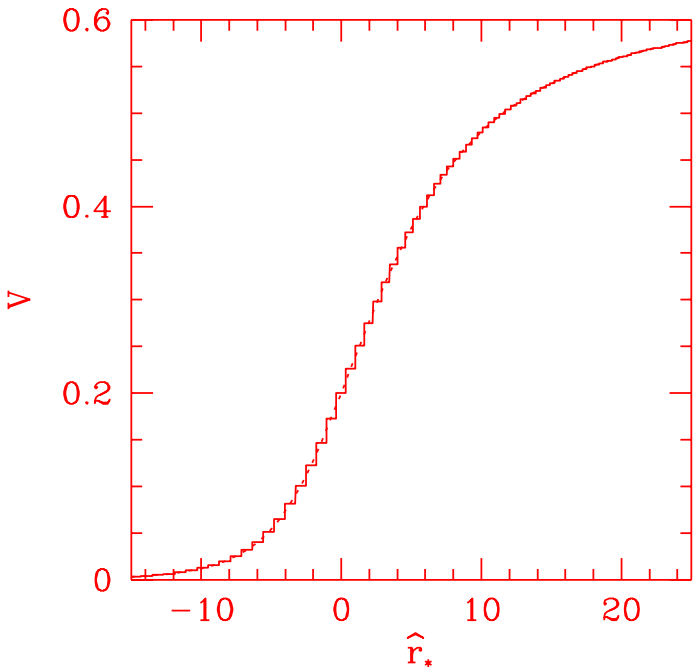


Fig. 1 : Behaviour of V_+ (smooth solid curve) for $a = 0.5$, $m_p = 0.8$, $\sigma = 0.8$. This is approximated as a collection of steps. In reality tens of thousand steps were used with varying step size which mimic the potential with arbitrary accuracy.

when energy of the wave is greater than the height of the potential barrier. The standard junction condition is given as [14],

$$Z_{+,n} = Z_{+,n+1} \quad \text{and} \quad \frac{dZ_+}{d\hat{r}_*}|_n = \frac{dZ_+}{d\hat{r}_*}|_{n+1}. \tag{25}$$

The reflection and transmission co-efficients at nth junction are given by:

$$R_n = \frac{A_{n+1}(k_{n+1} - k_n) + B_{n+1}(k_{n+1} + k_n)}{A_{n+1}(k_{n+1} + k_n) + B_{n+1}(k_{n+1} - k_n)}; \quad T_n = 1 - R_n \tag{26}$$

At each of the n steps these conditions were used to connect solutions at successive steps. Here, k is the wave number ($k = \sqrt{\sigma^2 - V_\pm}$) of the wave and k_n is its value at nth step. We use the 'no-reflection' inner boundary condition: $R \to 0$ at $\hat{r}_* \to -\infty$.

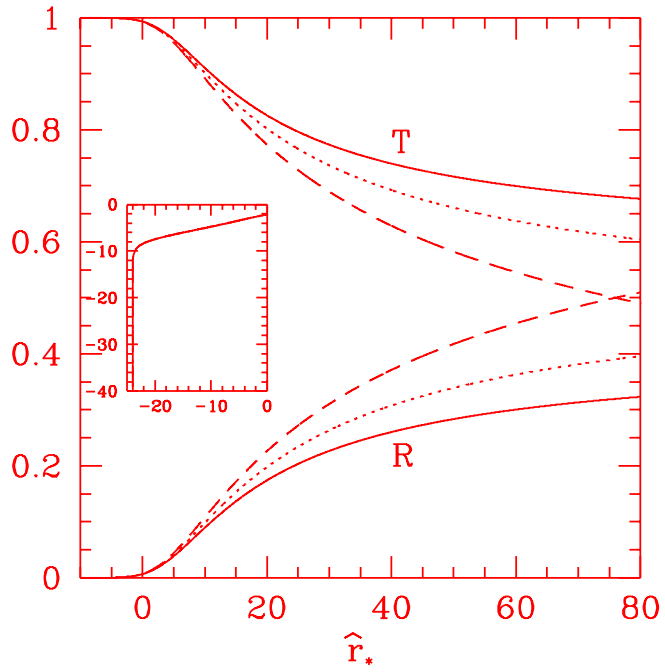


Fig. 2a: Reflection (R) and transmission (T) coefficients of waves with varying mass as functions of $\hat{r}_*$. $m_p = 0.78$ (solid), $m_p = 0.79$ (dotted) and $m_p = 0.80$ (long-dashed) are used. Other parameters are $a = 0.5$ and $\sigma = 0.8$. Inset shows R in logarithmic scale which falls off exponentially just outside the horizon.

For the cases where waves hit on the potential barrier, inside the barrier (where $\sigma^2 < V_+$) we use the wave function of the form

$$Z_{+,n} = A_n exp[-\alpha_n \hat{r}_{*,n}] + B_n exp[\alpha_n \hat{r}_{*,n}] \tag{27}$$

where, $\alpha_n = \sqrt{V_\pm - \sigma^2}$, as in usual quantum mechanics.

3. – Examples of Solutions

Fig. 2a shows three solutions [amplitudes of Re(Z_+)] for parameters: $a = 0.5$, $\sigma = 0.8$ and $m_p = 0.78,\ 0.79$, and 0.80 respectively in solid, dotted and long-dashed curves. The energy σ^2 is always higher compared to the height of the potential barrier (Fig. 1) and

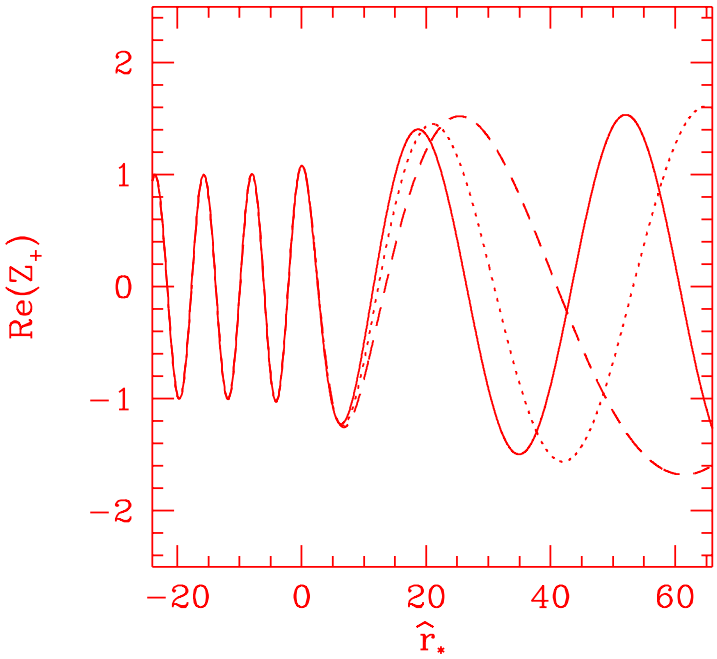


Fig. 2b: Amplitude of $\mathrm{Re}(Z_+)$ of waves with varying mass as functions of $\hat{r}_*$. $m_p = 0.78$ (solid), $m_p = 0.79$ (dotted) and $m_p = 0.80$ (long-dashed) are used. Other parameters are $a = 0.5$ and $\sigma = 0.8$.

therefore the particles do not 'hit' the barrier. k goes up and therefore the wavelength goes down monotonically as the wave approaches a black hole. It is to be noted that though ours is apparently a 'crude' method, it has flexibility and is capable of presenting insight into the problem, surpassing any other method such as ODE solver packages. This is because one can choose (a) variable steps depending on steepness of the potential to ensure uniform accuracy, and at the same time (b) virtually infinite number of steps to follow the potential as closely as possible. For instance, in the inset, we show R in logarithmic scale very close to the horizon. All the three curves merge, indicating that the solutions are independent of the mass of the particle and a closer inspection shows that here, the slope of the curve depends only on σ. The exponential dependence of R_n close to the horizon becomes obvious. Asymptotically, $V_\pm = m_p^2$ (eq. 22), thus, as m_p goes down, the wavelength goes down. In Fig. 2b, we present the instantaneous values of the reflection R and transmission T coefficients (i.e., R_n and T_n of Eq. 26) for the same three cases. As the particle mass is decreased, k goes up and corresponding R goes down consistent with the limit that as $k \to \infty$, there would be no reflection at all as in a quantum mechanical problem.

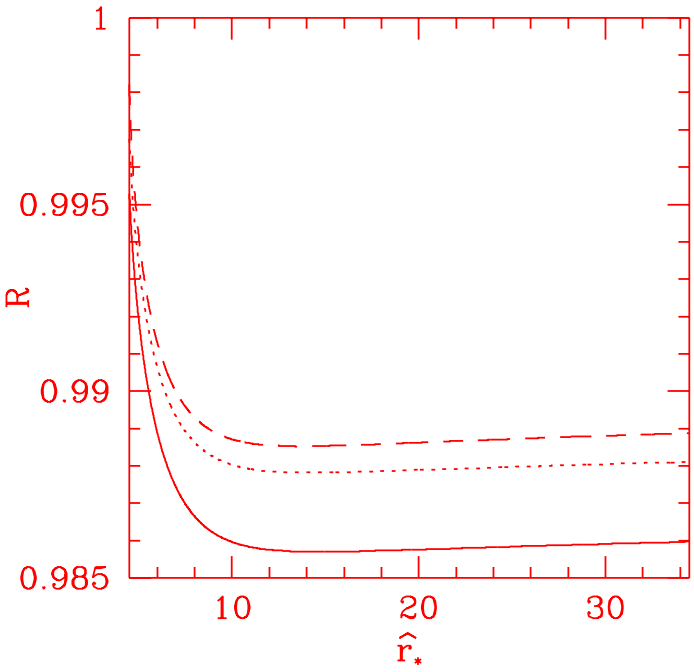


Fig. 3a: Reflection (R) coefficient of waves with varying mass as functions of $\hat{r}_*$. $m_p = 0.16$ (solid), $m_p = 0.164$ (dotted) and $m_p = 0.168$ (long-dashed) are used. Other parameters are $a = 0.95$ and $\sigma = 0.168$.

Figs. 3(a-b) compare a few solutions where the incoming particles 'hit' the potential barrier. We choose, $a = 0.95$, $\sigma = 0.168$ and mass of the particle $m_p = 0.16,\ 0.164,\ 0.168$ respectively in solid, dotted and long-dashed curves. Inside the barrier, the wave decays before coming back to a sinusoidal behaviour, before entering into a black hole. In Fig. 3b, we plotted the potential (shifted by 2.05 along vertical axis for clarity). Here too, the reflection coefficient goes down as k goes up consistent with the classical result that as the barrier height goes up more and more, reflection is taking place strongly. Note however, that the reflection is close to a hundred percent. Tunneling causes only a few percent to be lost into the black hole.

Figs. 4(a-b) show the nature of the complete wave function when both the radial and the angular solutions [7] are included. Fig. 4a shows contours of constant amplitude of the wave ($R_{-1/2}S_{-1/2}$) in the meridional plane – X is along radial direction in the equatorial plane and Y is along the vertical direction. The parameters are $a = 0.5$,

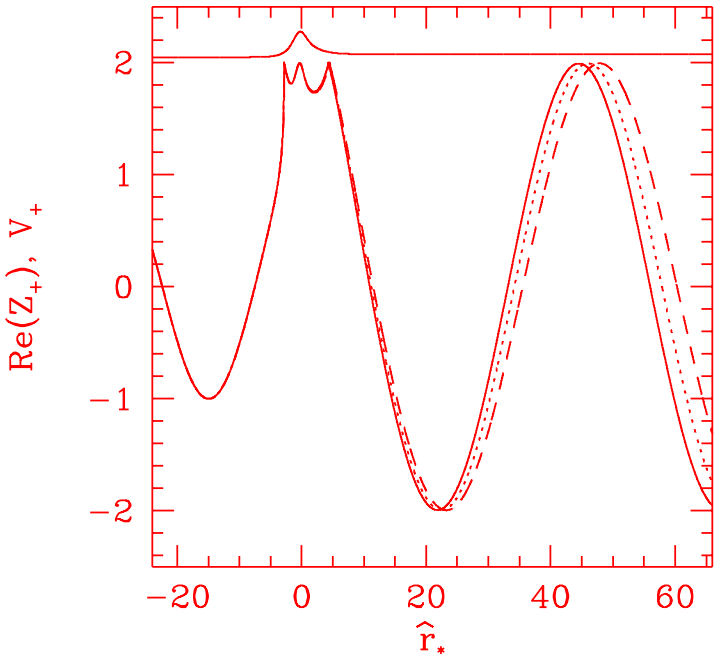


Fig. 3b: Amplitude of $\mathrm{Re}(Z_+)$ of waves with varying mass as functions of $\hat{r}_*$. $m_p = 0.16$ (solid), $m_p = 0.164$ (dotted) and $m_p = 0.168$ (long-dashed) are used. Nature of potential with $m_p = 0.168$ is drawn shifting vertically by 2.05 unit for clarity. Other parameters are $a = 0.95$ and $\sigma = 0.168$.

$m_p = 0.8$ and $\sigma = 0.8$. Some levels are marked. Two successive contours have amplitude difference of 0.1. In Fig. 4b a three-dimensional nature of the complete solution is given. Both of these figures clearly show how the wavelength varies with distance. Amplitude of the spherical wave coming from a large distance also gets weaker along the vertical axis and the wave is forced to fall generally along the equatorial plane, possibly due to the dragging of the inertial frame.

4. – Conclusion

We review here the scattering of massive, spin-half particles from a spinning black hole with particular emphasis to the nature of the radial wave functions and reflection and transmission coefficients. Here we presented a well known quantum mechanical step-

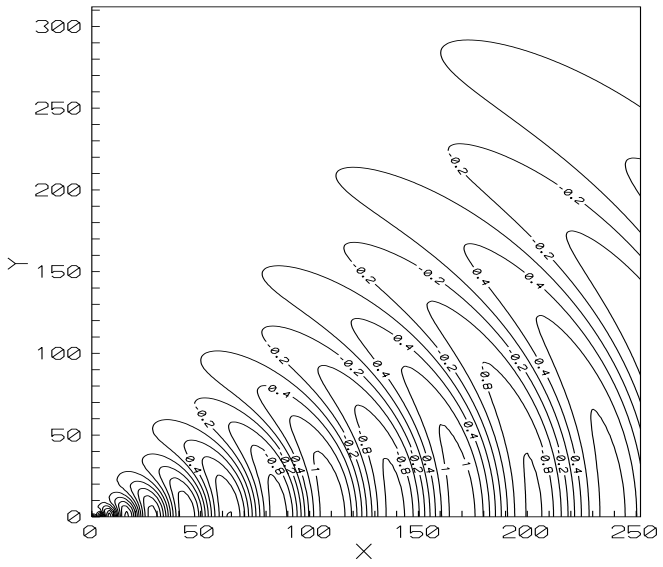


Fig. 4a: Contours of constant amplitude are plotted in the meridional plane around a black hole. Radial direction on equatorial plane is along X axis and the vertical direction and along Y. Both radial and theta solutions have been combined. Parameters are $a = 0.5$, $m_p = 0.8$ and $\sigma = 0.8$.

potential approach [10] but one can verify by any numerical technique that the solution would remain the same. A modified WKB approximation [8, 9, 11] also yields similar result in Kerr geometry [15]. The approach presented here (i.e., step potential approach) is very transparent since a complex problem of barrier penetration in a spacetime around a spinning black hole could be tackled very easily. We report a few significant observations of these papers that the wave function and R, and T behave similarly close to the horizon independent of the initial parameter, such as the particle mass m_p. Particles of different mass scatter off to a large distance completely differently, thus giving an impression that a black hole could be treated as a mass spectrograph! When the energy of the particle becomes higher compared to the rest mass, the reflection coefficient diminishes as it should it. Similar to a barrier penetration problem, the reflection coefficient becomes close to a hundred percent when the wave hits the potential barrier. Another significant observation is that the reflection and transmission coefficients are functions of the radial coordinates. This is understood easily because of the very nature of the potential barrier which is strongly space dependent which we approximate as a collection of steps. Combining with the solution of theta-equation, we find that the wave-amplitude

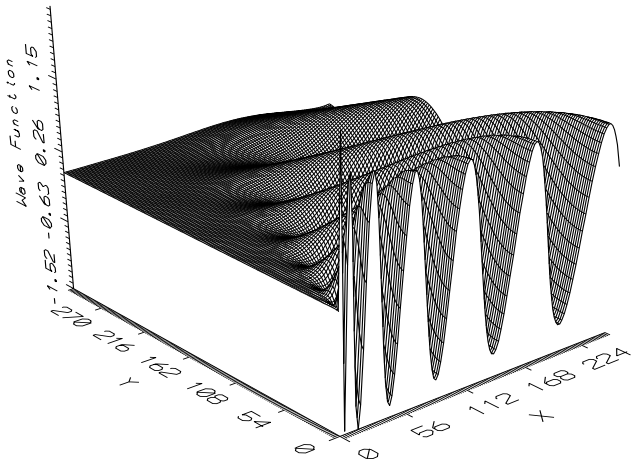


Fig. 4b: Three dimensional view of $R_{-1/2}S_{-1/2}$ are plotted in the meridional plane around a black hole. Both radial and theta solutions have been combined. Parameters are $a = 0.5$, $m_p = 0.8$ and $\sigma = 0.8$.

vanishes close to the vertical axis, possibly due to the frame-dragging effects.

REFERENCES

[1] Teukolsky S.,*Phys. Rev. Lett.*, **29** (1972) 1114.
[2] Teukolsky S.,*Astrophys. J.*, **185** (1973) 635.
[3] Chandrasekhar S.,*Proc. R. Soc. Lond. A*, **349** (1976) 571.
[4] Chandrasekhar S.,*The Mathematical Theory Of Black Holes*John Wiley: New York (1984).
[5] Press W. H.and Teukolsky S.,*Astrophys. J.*, **185** (1973) 649.
[6] Teukolsky S. and Press W. H.,*Astrophys. J.*, **193** (1974) 443.
[7] Chakrabarti S. K.,*Proc. R. Soc. Lond. A*, **391** (1984) 27.
[8] Mukhopadhyay B. and Chakrabarti S. K.,*Proceedings of the Mini-Workshop on Applied Mathematics* edited by Islam J. N., Hosain M. A., Rees D. A. S., Roy G. D. and Ghosh N. C. (Dept. of Mathematics, SUST) (1998) 251.
[9] Mukhopadhyay B. and Chakrabarti S. K.,*Class. Quant. Grav.*, **16** (1999) 3165.
[10] Chakrabarti, S.K. and Mukhopadhyay, B.,*Mon. Not. R. Astro. Soc.*, (2000) (submitted).
[11] Mukhopadhyay, B.,*Class Quant. Grav.*, (2000) (in press).
[12] Goldberg J. N., Macfarlane A. J., Newman E. T., Rohrlich F. and Sudarsan E. C. G., *J. Math. Phys.*, **8** (1967) 2155
[13] Breure R. A., Ryan M. P. Jr. and Waller S.,*Proc. R. Soc. Lond. A*, **358** (1982) 71.
[14] Davydov A. S.,*Quantum Mechanics* (New York: Pergamon Press) (1976).
[15] Mukhopadhyay B. and Chakrabarti S. K.,*Nuclear Physics B.*, (2000) (submitted).